Meson Captures in Solids*

M. Y. Au-Yang

Department of Physics, University of California, Berkeley, California

AND

Marvin L. Cohen†

Department of Physics and Inorganic Materials Research Division, Lawrence Radiation Laboratory, University of California, Berkeley, California

(Received 20 May 1968)

We present a calculation of the Z dependence of the atomic capture of negative mesons in simple compounds. We choose a self-consistent Fermi-Thomas potential and solve the resulting Schrödinger equation describing the meson in the solid. The results give better agreement with experiment than the Fermi-Teller linear Z law. The observed oscillatory behavior of the capture ratio as a function of Z for oxides is qualitatively explained.

I. INTRODUCTION

A DESCRIPTION of the capture processes of mesons in matter was first given about twenty years ago by Fermi and Teller.[1] Using simple models, they were able to argue that the capture probability for negative mesons in solids should be proportional to Z, the atomic number. Since that time, it has become possible to check the theoretical predictions experimentally, and although the results agree qualitatively with the theory, there are quantitative differences. The experimental results show that the capture probability[2] is not just linear in Z for all materials, but rather it appears to be proportional to Z^n, where $0.55 \leq n \leq 1.41$.

We mention, as an aside, that other discrepancies between experiment and theory existed. It was found[3] that the capture probability of π^- mesons by hydrogen in nuclear emulsions is much less than that of K^- mesons. This is contrary to what was expected on the basis of the theory of Fermi and Teller.[1] This problem has been discussed by Baker,[4] and he shows that the experimental results for hydrogen can be explained if one considers meson captures which arise from both radiative and Auger transitions.

In this work, we consider the Z dependence of the capture probability for negative mesons in solids. We begin by assuming that the solid can be represented by a collection of independent atoms and describe the scattering processes using this model. This model is appropriate for meson captures at energies above approximately 100 eV with the assumption that neither the mesons nor the electrons are in high-quantum-number states (i.e., large orbits). In this case the crystal potential, which affects only the high-quantum-number states and is of the order of 10 eV, can be ignored. This model has only limited validity.

In most systems, the captures occur below 100–500 eV, and the predominant mechanism is the Auger interaction with valence electrons causing meson transitions to high-quantum-number states. The "solid-state" effects are therefore important, i.e., the crystal potential and charge transfer effects are important. This conclusion is supported experimentally by comparing the capture ratios of two atoms in compounds to those in mixtures. For example, in the case of ZnS the value[5] is 1.7. To compute the effect of the crystalline potential, we compute the valence state wave functions for the mesons in a solid. Once these are obtained, we calculate the probability for the transition from these valence states to the localized atomic states in the same manner as was done for the noninteracting atoms case.

To compare the results with experiment, we consider binary compounds and compute the ratio of transitions into the low-lying localized states of the atoms. The matrix elements involved in this calculation are evaluated only approximately, and the capture ratio is evaluated at only two points in the Brillouin zone. It is found that the capture ratio depends weakly on $\mathbf{k}$ for compounds composed of atoms with low atomic numbers and can vary by about 30% for large atomic numbers. If a Brillouin-zone average is taken, the resulting ratios are in good agreement with experiment.

Finally, using simple models we are able to give a semiqualitative description of the periodic behavior of the capture ratios for oxides as a function of the positive-ion atomic number.

II. ISOLATED ATOMS MODELS

In this model, the transition probability R for the transitions of an unbound meson into all the bound

* Work supported by the National Science Foundation.

† Alfred P. Sloan Fellow.

[1] E. Fermi and E. Teller, Phys. Rev. 72, 399 (1947).

[2] J. S. Baijal, J. A. Diaz, S. N. Kaplan, and R. V. Pyle, Nuovo Cimento 30, 711 (1963).

[3] W. H. Barkas, J. N. Dyer, P. E. Giles, H. H. Heckman, C. J. Mason, N. A. Nickols, and F. M. Smith, Phys. Rev. 112, 622 (1958).

[4] G. A. Baker, Jr., Phys. Rev. 117, 1130 (1960).

[5] D. Jenkins (private communication).

states by means of Auger and spontaneous radiation processes are calculated. We assume hydrogenic states and allow all possible energy states of the unbound meson. The total transition rate for the meson as it is slowed down from the initial energy E_s (of order MeV in most experiments) to zero energy is then proportional to

$$\int_0^{E_s} \left(R \Big/ \frac{dE}{dx}\right) dE,$$

where dE/dx is the stopping power. In practice we can only calculate the rate R for a few values of the energy, and the integrand is interpolated between these values.

We will begin by finding dE/dx and the transition rates for radiative and Auger transitions. These will then yield the total rate and capture ratios.

The standard expression[6] for dE/dx is not accurate for very low energies. In the energy range where the meson has a velocity near or below that of the valence electrons, this expression no longer holds. For π^- and μ^- mesons with masses of approximately 200 electron masses, the lower limit of validity is about 10 keV. Below 10 keV we shall use a result due to Rosenberg.[7] In Rosenberg's treatment of this problem, the nucleus and the meson form a two-center potential for the electron, and the transition rates for the electron from a bound state to ionized states are calculated. The ionized state wave function is approximated by a free-particle wave function. This model was applied to the case of unit effective charge, $\bar{Z}=1$, of the nuclear center. However, for the low-energy region, the excitations of the valence electrons are mainly responsible for the energy loss ($\bar{Z}\cong 1$), so that the results for this case can be used provided we multiply the particle density N by the total number of valence electrons for each atom, n. Rosenberg obtained an expression for the stopping power as a function of meson velocity v, in terms of a function $g(v)$:

$$-dE/dx = Nng(v), \tag{1}$$

and he computed $g(v)$ numerically for $v\leq 1$. The value $v=1$ corresponds to a meson having $(13.6\times M)$ eV, $M=$mass of meson in m_e. His results are valid only for low energies. We shall see that for most materials, all significant captures occur below $(13.6\times M)$ eV, and so the above curve covers the entire range of interest.

We shall be interested in the function

$$1/\,|\,(dE/dx)\,(E)\,|,$$

and we therefore define

$$f(E)=g(v)$$

and

$$Q(E)=\,|\,dE/dx\,|^{-1}=[Nnf(E)]^{-1}. \tag{2}$$

The function $1/f(E)$ is plotted in Fig. 1.

We now calculate the transition rate W in the dipole approximation for the scattering of a meson in a mesonic plane-wave state to one of the mesonic atomic states by radiative process,

$$W=(4e^2\omega^3/3\hbar c)\;|\;\mathbf{r}_{if}\;|^2, \tag{3}$$

where ω is the energy between the initial and final states, and $\mathbf{r}_{if}$ is the dipole matrix element between these states. We shall use hydrogenlike wave functions for the mesonic atomic states, we consider this to be a rough approximation for two reasons: first, the high-lying states (large radii) interact strongly with the electrons; second, for large nuclei, the nuclear penetration of the mesonic wave function produces a large correction to the point-nucleus approximation.

The initial state for a particle in the Coulomb field is

$$\Psi_i=C_k(\mathbf{r})/L^{3/2}, \tag{4}$$

where $C_k(\mathbf{r})$ is the Coulomb wave function,[8] and the final state is

$$\psi_f=Y_l^m(\theta,\phi)\mathfrak{R}_{nl}(r), \tag{5}$$

where

$$\mathfrak{R}_{nl}(r)=-\left\{\left(\frac{2ZM}{na_0}\right)^3\frac{(n-l-1)\,!}{2n[(n+l)\,!]^3}\right\}^{1/2}e^{-\rho/2}\rho^l L_{n+l}^{2l+1}(\rho),$$

$$L_{n,l}^{2l+1}(\rho)=\sum_{k=0}^{n-l-1}(-1)^{k+1}\frac{[(n+l)\,!]^2\rho^k}{(n-l-1-k)\,!\,(2l+1+k)\,!k!},$$

$$\rho=(2ZM/na_0)r, \quad \text{and} \quad M=M_{\text{meson}}/m_e.$$

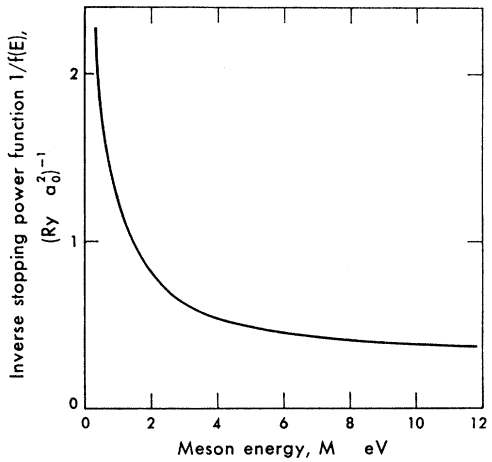

FIG. 1. The inverse stopping power function $\{f(E)\}^{-1}$ as a function of the incident meson energy. M is the mass of the meson in units of electron mass.

[6] J. D. Jackson, *Classical Electrodynamics* (John Wiley & Sons, Inc., New York, 1962), p. 429.

[7] R. L. Rosenberg, Phil. Mag. **40**, 759 (1949).

[8] G. Breit, in *Tables of Coulomb Wave Functions, U.S. National Bureau of Standards, Applied Mathematics Series-17* (U.S. Government Printing Office, Washington, D.C., 1952), Vol. I.

To calculate the matrix element of the radius vector we will let $\mathbf{k}$ be parallel to $\hat{z}$, so that we have[8]

$$C_k(\mathbf{r}) = \sum_{l'=0}^{\infty} (2l'+1) i^{l'} C_{l'}(kr) P_{l'}(\cos\theta), \qquad (6)$$

where

$$C_l(kr) = \frac{e^{i\sigma_l} F_l(\eta; kr)}{kr},$$

$$\sigma_l = \arg \Gamma(l+1+i\eta),$$

$$F_l(\eta; \rho) = S_l e^{i\rho} \rho^{l+1} F(l+1+i\eta \mid 2l+2 \mid -2i\rho),$$

$$S_l = 2^l e^{-\pi\eta/2} \frac{\mid \Gamma(l+1+i\eta) \mid}{(2l+1)!}, \qquad \eta = -MZe^2/\hbar^2 k,$$

and $F(d \mid \beta \mid Z)$ is a confluent hypergeometric function. This gives

$$\mathbf{r}_{if} = A \sum_{l'=0}^{\infty} (2l'+1) i^{l'} \sum_{k=0}^{n-l-1} (-1)^k \times [(n-l-1-k)!\, k!\, (2l+1+k)!]^{-1} \times \int Y_l^m(\theta, \phi) P_{l'}(\cos\theta)\, \mathbf{r} \times \int \rho^{l+k} C_{l'}(\rho k n a_0/2MZ) e^{-\rho/2} \rho^2 d\rho\, d\Omega, \qquad (7)$$

where

$$A = \frac{1}{L^{3/2}} \left\{ \left(\frac{2ZM}{na_0}\right)^3 \frac{(n-l-1)!(n+l)!}{2n} \right\}^{1/2} \left(\frac{na_0}{2MZ}\right)^4.$$

The integral is a product of a radial and an angular integral. The radial integral is

$$\mathfrak{R} = \int_0^{\infty} \rho^{l+k+3} C_{l'}(kna_0\rho/2MZ) e^{-\rho/2} d\rho \qquad (8)$$

and the angular integral is

$$I = \int_0^{2\pi} \int_{-1}^{1} P_{l'}(\cos\theta)\, Y_l^m(\theta, \phi) \times \begin{Bmatrix} \cos\theta & \\ \sin\theta & \cos\phi \\ \sin\theta & \sin\phi \end{Bmatrix} d(\cos\theta)\, d\phi, \qquad (9)$$

where the three entries of the matrix correspond to each component of the radius vector, z, x, y.

The angular integral is a product of three spherical harmonics, and its value in terms of Clebsch-Gordan coefficients is given by Edmonds.[9] The most general form of the radial integral can be written as

$$J = \int_0^{\infty} C_l(kr) e^{-r} r^n dr, \qquad (10)$$

where n is an integer greater than 2. This integral must be evaluated numerically, and to do this we need to know the properties of C_l. As expected, for large values of kr, C_l exhibits the characteristic oscillating behavior of $j_l(kr)$; in fact

$$C_l \sim (e^{i\sigma_l}/kr) \sin[kr - \eta \ln(2kr) - \tfrac{1}{2}(l\pi) + \sigma_l] \qquad (11)$$

for

$$kr \gg (l+1)l + \eta^2.$$

The general behavior of C_l as a function of kr from 0 to ∞ can be roughly described in the following way: For $kr \ll 1$, C_l increases as $(kr)^l$, then as kr gets larger, C_l increases more rapidly until $kr = \eta + [\eta^2 + l(l+1)]^{1/2}$; after this point, C_l oscillates and goes to the asymptotic expression above. The behavior of $C_l(kr)$ is therefore very similar to that of $j_l(kr)$, except that oscillations do not start until

$$kr = \eta + [\eta^2 + l(l+1)]^{1/2}. \qquad (12)$$

Because of these oscillations the numerical evaluation of J is difficult for large values of n or k. In practice, with the storage available in the CDC 6600 computer, n is limited to about 30 for k very near to zero (i.e., mesons with energies less than about 1 keV).

For Auger transitions, we treat the Coulomb repulsion between the electron and the meson as a perturbation on the system and find the transition rate for going from a free meson, bound electron state to a free electron, bound meson state. We shall neglect all other excitations of the electron except ionization.

We use time-dependent perturbation theory and the transition rate is

$$W = (2\pi/\hbar) \mid H_{if}' \mid^2 \rho. \qquad (13)$$

The initial state is $\bar{C}_{k_1}(\mathbf{r}_1)/L^{3/2}$ for the meson, and $\Psi_{\bar{n}\bar{l}\bar{m}}(\mathbf{r}_2)$ for the electron, and the final meson state is $\bar{\psi}_{n'l'm'}(\mathbf{r}_1)$, where the bar indicates a wave function in which the electron mass is replaced by the meson mass. The final electron state is $C_{k_2}(\mathbf{r}_2)/L^{3/2}$. The momentum of the final free electron is $\mathbf{k}_2$ and $\mathbf{k}_1$ is the momentum of the initial free meson. The transition matrix element becomes

$$H_{if}' = (e^2/L^3) \int \Psi_{\bar{n}\bar{l}\bar{m}}^*(\mathbf{r}_2) \bar{C}_{k_1}^*(\mathbf{r}_1) \times \mid \mathbf{r}_1 - \mathbf{r}_2 \mid^{-1} \bar{\psi}_{n'l'm'}(\mathbf{r}_1) C_{k_2}(\mathbf{r}_2) d^3r_1 d^3r_2, \qquad (14)$$

and $\mathbf{k}_2$ and $\mathbf{k}_1$ are related by energy conservation:

$$\frac{\hbar^2 k_2^2}{2m_e} - \frac{Z^2 e^2 M}{2a_0 n'^2} = \frac{\hbar^2 k_1^2}{2Mm_e} - \frac{Z^2 e^2}{2a_0 \bar{n}^2}, \qquad (15)$$

[9] A. R. Edmonds, *Angular Momentum in Quantum Mechanics* (Princeton University Press, Princeton, N.J., 1960), p. 63.

where

$$M = M_{\text{meson}}/m_e, \qquad \text{as before.}$$

We note that for some values of k_1 and $\bar{n}$, there is a maximum allowed n'. Using this expression

$$|\mathbf{r}_1 - \mathbf{r}_2|^{-1} = 4\pi \sum_{l=0}^{\infty} \sum_{m=-l}^{l} \frac{r_<^l}{r_>^{l+1}} (2l+1)^{-1} Y_l^{m*}(\theta_1, \phi_1) Y_l^m(\theta_2, \phi_2), \tag{16}$$

and taking $\mathbf{k}_1$ as the direction of $\hat{z}$,

$$\bar{C}_{\mathbf{k}_1}(\mathbf{r}_1) = \sum_{l'=0}^{\infty} (2l'+1) i^{l'} \bar{C}_{l'}(k_1 r_1) P_{l'}(\cos\theta_1); \tag{17}$$

$$C_{\mathbf{k}_2}(\mathbf{r}_2) = 4\pi \sum_{l'=0}^{\infty} \sum_{m'=-l'}^{l'} i^{l'} C_{l'}(k_2 r_2) Y_{l'}^{m'*}(\theta_{k_2}, \phi_{k_2}) Y_{l'}^{m'}(\theta_2, \phi_2). \tag{18}$$

The matrix element becomes

$$H_{if}' = \frac{(4\pi e)^2}{L^3} \sum_{l=0}^{\infty} \sum_{m=-l}^{l} \sum_{k=0}^{\infty} \sum_{l''=0}^{\infty} \sum_{m''=-l''}^{l''} (-1)^k \times \frac{(2k+1)}{(2l+1)} i^{k+l''} \int \frac{r_<^l}{r_>^{l+1}} \bar{C}_k^*(k_1 r_1) \times C_{l''}(k_2 r_2) R_{\bar{n}\bar{l}}(r_2) \bar{R}_{n'l'}(r_1) d^3r_1 d^3r_2 \times \int Y_l^{m*}(\theta_1, \phi_1) Y_l^m(\theta_2, \phi_2) \times P_k(\cos\theta_1) Y_{l''}^{m''}(\theta_2, \phi_2) Y_l^{\bar{m}*}(\theta_2, \phi_2) Y_{l'}^{m'}(\theta_1, \phi_1) d\Omega_1 d\Omega_2 Y_{l''}^{m''*}(\theta_{k_2}, \phi_{k_2}). \tag{19}$$

The angular integrals are again expressible in terms of Clebsch-Gordan coefficients. We need not consider the angular part of $\mathbf{k}_2$ since we shall be integrating over all directions after squaring the matrix element. The radial integral is again done numerically.

These expressions allow us to calculate the radiative and Auger transition rates for a meson density of one meson per L^3 on one atom, and we need now to apply these results to the experimental situation in which a beam of mesons is used.

Consider a meson beam with initial energy E_s moving in the $\hat{z}$ direction (with a flux of 1 particle per sec Å^2) impinging on a solid with N_i atoms of type i per Å^3. We consider only one-to-one binary compounds, so that $i=1,2$ and $N_1=N_2=N$. For convenience we take the solid in the form of a rod in $\hat{z}$ direction of cross-sectional area A square angstroms. Let $R_i(E)$ be the total transition rate (Auger plus radiative) for meson density of 1 particle per Å^3 and for one scattering center of type i, and $C_i(E)$ be the corresponding number of captures per Å^3. Define the grand total transition rate $R=R_1+R_2$, and the total captured meson density $C=C_1+C_2$. Let $P(E)$ be the meson beam density (per Å^3) and $v(E)$ be the velocity of the meson. The energy E, at any point along the rod, is taken to be the average energy per meson of the beam at that point. We note that there is a one-to-one correspondence between the distance along the rod z and the energy E.

Consider a small length Δz of the rod at z (energy E); the corresponding change in energy is $-\Delta E$. Now the total rate of capture for *one* atom type i is PR_i, and the total number of atoms of type i in the length Δz is $NA\Delta z$. The total rate of capture Ω_i by all the atoms of type i in the length Δz is, therefore,

$$\Omega_i = PR_i NA\Delta z = -PR_i NAQ\Delta E. \tag{20a}$$

But

$$\Omega_i = (\Delta C_i/\Delta t)\Delta z A = Av\Delta C_i. \tag{20b}$$

Combining Eqs. (20a) and (20b) we have, in the limit of small changes,

$$v dC_i = -NR_i PQ dE. \tag{21}$$

The two equations (21), $(i=1, 2)$, are to be solved simultaneously subject to the three boundary conditions

$$P(E) = (1/v_s A) - C(E), \qquad C_1(E_s) = C_2(E_s) = 0. \tag{22}$$

The term $1/(v_s A)$ is the initial density of the meson beam. Therefore, the first condition expresses the conservation of the number of mesons at any point along the rod. The last two conditions merely state that at the initial energy (the initial end of the rod) no mesons have been captured by either atom type. The coupled equations (21) subject to Eqs. (22) have the solution

$$\bar{C}_1 = A \int_E^{E_s} (NR_1 Q/v) \exp\left\{-N \int_E^{E_s} (QR/v) dE\right\} dE, \tag{23}$$

$$\bar{C}_2 = B \int_E^{E_s} (NR_2 Q/v) \exp\left\{-N \int_E^{E_s} (QR/v) dE\right\} dE, \tag{24}$$

with

$$\bar{C}_1 + \bar{C}_2 = v_s^{-1}\left[1 - \exp\left\{-N \int_E^{E_s} (QR/v) dE\right\}\right], \tag{25}$$

where A and B are constants to be determined by using Eq. (25), and $\bar{C}_i = \bar{C}_i A$ is the capture per unit length by type i atoms.

It is easily seen that the fraction captured at any E is given by the exponential term of Eq. (25). If this term is small compared to unity, then most of the beam is captured when the beam energy is reduced to this value of E and Eqs. (23) and (24) can be used to find the ratio of captures by the two types of atoms.

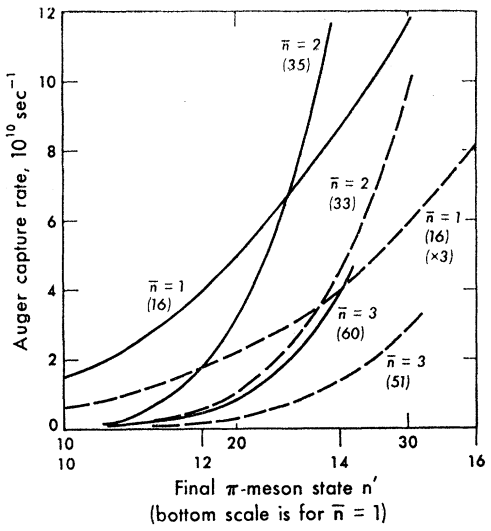

FIG. 2. Auger transition rates for Zn and S as a function of the final π meson states n', for various initial electron states $\bar{n}$. The calculations are for initial electron states with $\bar{l}=0$, but the nonzero-$\bar{l}$ states do not contribute much to the transitions. The maximum allowable n' for each value of $\bar{n}$ is shown in parentheses. The initial meson energy is 100 eV. Broken curves are for Zn and full curves are for S.

We note that the theory in this section can be compared with experimental numbers quantitatively only if most captures involve *low*-lying states of both electrons and mesons, so that the individual-atom theory holds, as stated earlier.

Typical results are shown in Figs. 2–5. We shall discuss them individually. All the rates (R) shown are in sec^{-1}, using $L=1$ Å.

In Fig. 2, the Auger transition rates are given for Zn and S. These are typical of rate versus meson quantum number n' for various electron quantum $\bar{n}$ curves. We see that the largest contribution to the capture comes from the largest allowed n', i.e., from high-lying states. Since our computations are good only for n' smaller than about 30, and for most atoms of interest the highest allowed n' (limited both by the size of the atom and also by energy conservation) is about 40 to 70, we see that the capture rate for Auger processes can only be obtained by extrapolation. In addition, we also expect that the individual-atom theory will break down.

In Fig. 3, the radiative transition rates calculated for Zn and S are given, and again these are typical of rate-versus-n' curves for most materials. In contrast to the Auger rates, the largest contributions come from the smallest values of n' (except $n'=1$). The largest rate for a single transition is about one order of magnitude larger than that for an Auger process; however, the rate quickly drops down for higher n''s. Because of this, the total Auger contribution is about one order of magnitude larger than the total radiative contribution. Note that the rate for $n'=1$ is a few orders of magnitude smaller than that for $n'=2$. This arises from the fact that the $n'=1$ state has no $1'\neq 0$ contribution.[10] Baker[4] stated that the radiative capture cross section is much smaller than electron ejection capture cross section by calculating only the $n'=1$ case, and, because of the above considerations, this statement does not seem to be justified.

In Fig. 4, the energy dependence of the Auger and radiative rates are given. We see that both rates decrease as the energy increases, and the radiative rate drops much more rapidly, making it much less important in its contribution to the captures.

Figure 5 contains a plot of the integrand of Eq. (25), and only the Auger contribution is included. We see that this function decreases extremely rapidly with increasing energy. This arises from the fact that all of the three factors $R(E)$, $Q(E)$, and $1/v(E)$ decrease with increased E. Numerically, we find [using Eq. (25)] that most captures occur between 100 and 500 eV. From Fig. 5 we see that by taking E_s to be 500 eV or above involves an error of less than 10%. We remark that if radiative contributions are neglected and we assume that $R_A(E)$ curve is the same except for normalization for both elements in the compound, then the ratio of capture is just the ratio of capture rates at any E, say $E=100$ eV, as is easily verified using Eqs. (23) and (24). Such a procedure is applicable

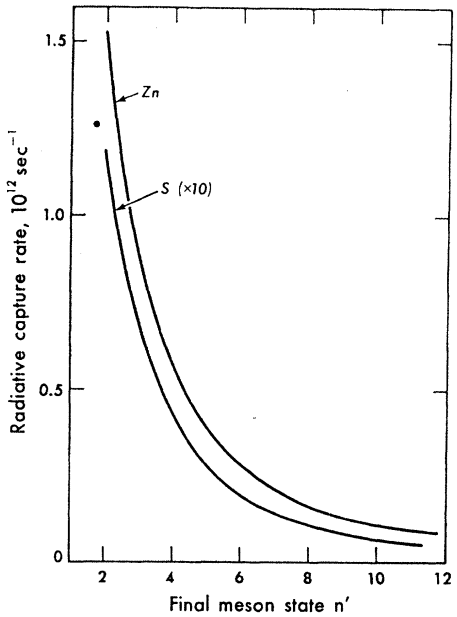

FIG. 3. Radiative transition rates for Zn and S as a function of the final π meson states n', for initial meson energy of 100 eV. The rate for $n'=1$ is not shown because it is a few orders of magnitude smaller.

[10] If the initial energy E of the meson is so small that its wavelength is much larger than (a_0/MZ), then the radiative transition rate for $l=0$ goes as E, whereas that for $l\neq 0$ goes as a constant. This value of energy is much larger than 100 eV.

here, but as stated above, the results obtained are limited in their application to experiment.

We conclude this section by discussion the history of a beam of mesons in a solid from the point it enters into its capture. In a typical experiment, the incoming meson has energies of the order of MeV, and its range is thus about a few tenths of a cm. For most of its range, it is slowed down by its interaction with electrons. Only during the final micron of its range does significant capture take place. At this state its velocity is about that of the valence electrons, and so the meson-electron interaction has the largest cross section in this region and the mesons are captured into high-lying mesonic states. By the time the average beam energy has been reduced to about 100 eV, most of the beam is captured, and from these initial captured states, the mesons cascade down to the lower states.

Experimentally, the determination of the number of meson captures by two elements in a simple compound is made by measuring the characteristic x-rays produced by the mesons as they cascade between *low*-lying states (with n less than 10), and a detailed study of the cascade is necessary. However, the determination of the ratio of the captures requires only the cascade rates from the "valence" states to the two sets of "core" states. The terminology of valence and core states comes from the analogy with electron states; admittedly, here they are not well defined because the Pauli exclusion principle is not applicable. We shall, however, use these terms to denote *nonlocalized* and *localized* bound states in the solid, which we shall define only by the size of the orbit.

III. REAL SOLIDS—INTERACTING ATOMS MODEL

The Schrödinger equation is

$$[-(\hbar^2\nabla^2/2m)+V(\mathbf{r})-E(\mathbf{k})]\Psi(\mathbf{k},\mathbf{r})=0. \quad (26)$$

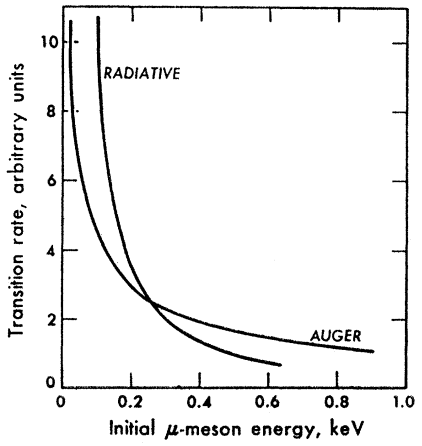

FIG. 4. The dependence on the initial meson energy of the Auger and radiative transition rates.

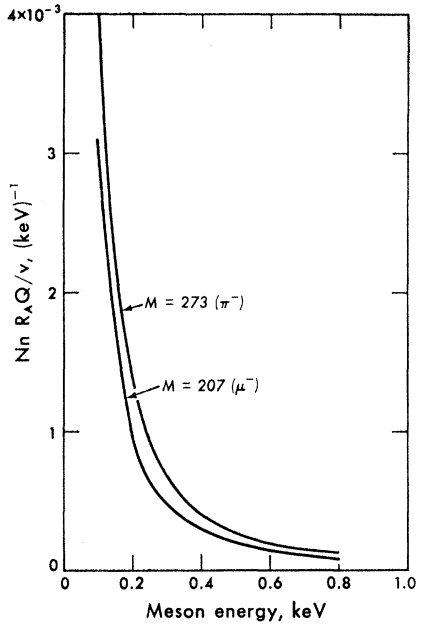

FIG. 5. The energy dependence of the integrand of Eq. (25) assuming only Auger processes for $\bar{n}=1$, $n'=16$, $Z=30$, and using Fig. 4.

To solve Eq. (26) we divide the unit cell of the compound into N Wigner-Seitz cells, where N is the number of atoms in the cell. We will assume that the atoms (or rather ions) are of the same size. We define

$$\Psi_p(\mathbf{k},\mathbf{r})=\exp(-i\mathbf{k}\cdot\mathbf{p})\Psi(\mathbf{k},\mathbf{r}), \quad (27)$$

where $\mathbf{p}$ locates the origin of the pth polyhedron and because of the Bloch condition,[11] Ψ_p is the same for equivalent polyhedrons of different unit cells. The continuity of the wave functions across the boundaries of polyhedrons now require that

$$\Psi_p(\mathbf{k},\mathbf{r})=\exp[-i\mathbf{k}\cdot(\mathbf{p}-\mathbf{q})]\Psi_q(\mathbf{k},\mathbf{r}),$$
$$\nabla\Psi_p(\mathbf{k},\mathbf{r})=\exp[-i\mathbf{k}\cdot(\mathbf{p}-\mathbf{q})]\nabla\Psi_q(\mathbf{k},\mathbf{r}) \quad (28)$$

for all p,q and at all points on the boundary between two polyhedrons labeled by p and q. If we require the potentials at each p site, $V_p(\mathbf{r})$, to be spherically symmetric, i.e., $V_p(\mathbf{r})=V_p(r)$, then Eq. (26) can be solved in each polyhedron since it is now separable, and we can write

$$\Psi_p(\mathbf{r})=\sum_{s=0}^{\infty}A_{ps}\phi_{ps}(\mathbf{r}_p,\lambda), \quad (29)$$

where

$$\phi_{ps}(\mathbf{r}_p,\lambda)=L_s(\theta_p,\phi_p)P_s(r_p,\lambda). \quad (30)$$

The functions $L_s(\theta_p,\phi_p)$ are lattice harmonics which are linear combinations of spherical harmonics of order

[11] M. Tinkham, *Group Theory and Quantum Mechanics* (McGraw Hill Book Co., New York, 1964), p. 268.

s. These are completely specified by the symmetry of the lattice and are determined by expressions of the form

$$R_j[L_s^m]=[L_s^m][\Gamma_j^m], \tag{31}$$

where $R_j \in$ (group of the wave vector $\mathbf{k}$), and Γ_j^m is the mth irreducible representation of R_j.

The functions $P_s(r_p, \lambda)$ are solutions of the radial equation

$$[-(\hbar^2/2m)\nabla_r^2+V(r_p)+l(l+1)/r_p^2-\lambda]P_s(r_p, \lambda)=0, \tag{32}$$

where λ is the energy eigenvalue. Thus the determination of the wave function reduces to three processes: (1) finding the lattice harmonics for a given symmetry, (2) solving for P_s after finding the appropriate $V(r_p)$, and (3) applying the conditions Eq. (28) to determine the coefficients in Eq. (29). We shall proceed in this order.

We can use the defining relations to compute the coefficients for the lattice harmonics expansion. However, for a variety of crystal structures, this has been done[12] and we shall simply use the results. For simplicity we shall only consider $\mathbf{k}=0$ and $\mathbf{k}=(\pi/a)(1, 0, 0)$ and consider only s waves. This should give a representative eigenfunction of the Schrödinger equation (26), and should not differ grossly from the average eigenfunction.

For usual band-structure calculations for electrons, the potential can be calculated or fit to experiments. However, for the meson case, the potential felt by the meson is different from that felt by an electron, because the Pauli exclusion principle is not applicable. In this case, to get calculations which are manageable, we approximate the potential by a sphericalized Fermi-Thomas potential.[13]

The effects of charge transfer (the Madelung potential) should also be taken into account. The simplest way to do this is to estimate the charge transfer by the effective charge parameter (or the amount of ionic character[14] times the number of valence electrons) Z_f. We shall simply use this parameter and the Madelung constant for agiven symmetry to give the Madelung potential. The effect of this on the Fermi-Thomas potential can be simply thought of as an ion having Z_f unscreened charged and $Z-Z_f$ screened charges if the ion is positive, and $-Z_f$ unscreened charges and $Z+Z_f$ screened charges if the ion is negative. This neglects the redistribution of the electrons, but serves as a first-order correction to the potential of the atom in the solid state. The parameter Z_f is obtained from Pauling.[14] His empirical form for the ionic character fits the measurements of the dipole moments of the compounds and it thus gives a good approximation to the parameters needed.

The potential obtained in this manner cannot be expressed as a simple function and it is therefore used in a tabulated form.

Having obtained the potential we can now solve the radial equation. It can be written as (at any site p)

$$(d^2X_l/dr^2)+f_l(r)X_l=0, \tag{33}$$

where $X_l=rP(r)$ and $f_l(r)=(2m/\hbar^2)(\lambda-V(r))-[l(l+1)/r^2]$. This equation can be solved numerically, but before solving it we note that since the meson is about 200 times the mass of the electron, the equation is similar to that for the electron except that the potential is multiplied by a factor of 200. Thus we see that, depending on the sign of the function $f(r)$, the wave function either oscillates very rapidly (f is positive), or is damped out very rapidly (f is negative). This is consistent with our understanding of the mesonic atom, since we know that for equal energies, the electron state has a much smaller principal quantum number n than the meson, i.e., the meson wave function is much more oscillatory.

The fact that we are essentially dealing with an electron in a huge potential brings out a problem which is not usually encountered in band-structure calculations: numerical methods are difficult since the wave function in high-lying atomic states depends very sensitively on the conditions imposed at the origin. (Numerical solutions of differential equations usually result from a scheme of generating the solutions from one point.) It is generally impossible to specify the correct condition at the origin to give an exponentially *damped* wave function f far from a given point. A different method must be used. We used here the WKB approximation. It is used in its region of validity, $|f'| \ll |f^{3/2}|$, and other numerical methods are used when this condition is not satisfied.

One more simplification is made. Since we are only interested in states which are localized near the surface of the ions, and since we know also that the wave function is damped out very rapidly for $f(r)$ having negative values, then if λ is an energy eigenvalue for a valence state $f(r)$ must be negative only very near the surface. Now the region of zero potential is not clearly defined and we may neglect it and assume that the ion's edge lies at $f=0$.

To use the expansion [Eq. (29)], we truncate and limit the largest value of the angular momentum to some number L. The expansion itself will then contain n constants to be determined, where n is the number of nonvanishing lattice harmonics below $L+1$. The total number of constants for a two-ion compound is then $n+n'-1$, where n, n' correspond to the two ions; the absolute normalization is unimportant.

[12] D. G. Bell, Rev. Mod. Phys. **26**, 311 (1954).
[13] V. Bush and S. Caldwell, Phys. Rev. **38**, 1898 (1931).
[14] L. C. Pauling, *The Nature of the Chemical Bond and the Structure of Molecules and Crystals* (Cornell University Press, Ithaca, N.Y., 1960), 3rd ed.

We now choose a few points on the boundary of the two ions, and apply the conditions Eq. (28), which become for $k=0$ simply the continuity of the wave function and its gradient across the interface. The number of independent points N (some points are related by symmetry) must be such that it satisfies

$$4N \gg n'+n-1,$$

since there are four equations for each point and we must have an overdetermined set of equations to solve the eigenvalue equation. The actual determination of the eigenvalues involves varying the energy parameter λ, and for each λ a least-squares fitting procedure is applied. The best fit will then indicate the presence of an eigenvalue. The $n+n'-1$ constants are also determined at the same time.

In actual calculations, we used $L=4$, and for both the zinc blende and the sodium chloride structure at $\mathbf{k}=0$, $n'=n=2$ and so it is assumed that $N=5$ is sufficient. [For $\mathbf{k}=(\pi/a)(1, 0, 0)$, $L=3$ to give $n=n'=2$.]

It is to be noted that we do not take proper account of the valence character of the electrons. This affects our calculations in two important ways: (1) through the potential that the meson valence wave function feels and (2) the interactions with the meson, i.e., cascade processes. The first objection is not as serious as the second for two reasons. The potential arising from other electrons is large compared with that from the valence electrons for most of the volume of the atom, and our calculation involves a sphericallized potential, which tends to smooth out the details of the potential from valence electron screening. The second objection is more serious; however, calculations show that for heavier atoms in most of the regions where the meson amplitude is large, the contribution of the other electrons to the total electron density is larger than that from the valence electrons. In fact, the Fermi-Thomas atom contains only half the total electrons within a radius of $(1.33/Z^{1/3})a_0$.

In Table I, we tabulate our calculated results and compare them with experiment. We note that the number of compounds calculated are few compared with the data available. This is because of the three limitations of our model: (1) The compound must be one-to-one binary, (2) it must have a simple structure (we consider only NaCl, Zn blende, and CsCl), and (3) the ions must have about equal size. A qualitative comparison with *all* the data is to follow.

TABLE I. The capture ratios of some compounds. Comparison of the calculated to the experimental and also the Z-law values.

Compound	Z ratio	Calculated ratio	Experimental ratio	Reference
ZnS	1.87	3.0	2.6±0.4	a
AgI	0.89	1.9	1.5±0.2	b
MgO	1.5	0.82	0.83±0.1	b
CaO	2.5	1.6	1.4±0.1	b
CdO	6.0	6.0	6.7±1.5	b

[a] Reference 5.
[b] Reference 15.

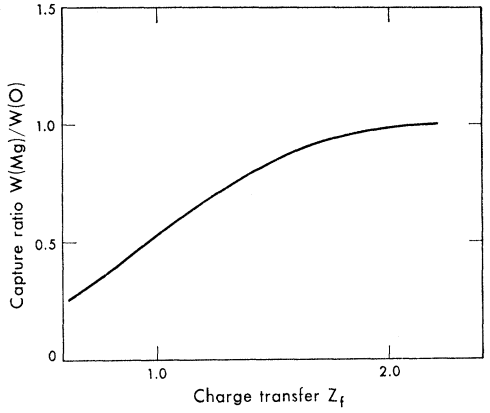

FIG. 6. The variation of the capture ratio with the charge transfer parameter Z_f for MgO.

Zinov *et al.*[15] noted that the capture ratio for the oxides as a function of the atomic number of the positive ion follows a periodic pattern as a function of atomic number. Because of the restrictions on our model we are not able to calculate all the ratios which are obtained experimentally; we can qualitatively explain the periodicity using our model. It is reasonable to expect that the parameter which produces the periodicity is Z_f, the effective charge transfer. If we look at Table 3.8 of Pauling,[14] we see that the electronegativity is periodic in atomic number.

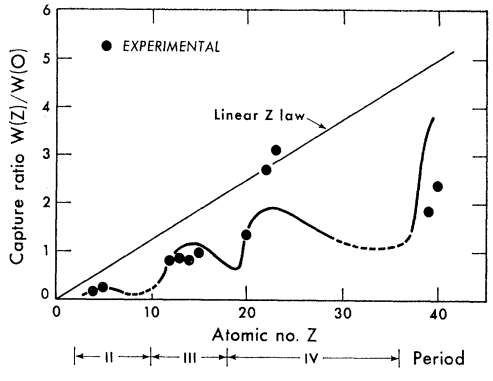

FIG. 7. Schematic plot of the capture ratio of oxides as a function of the atomic number Z of the positive ion, assuming a linear Z-law background, and using Fig. 6. The plot is normalized for MgO. Experimental values from Ref. 15 are included for comparison.

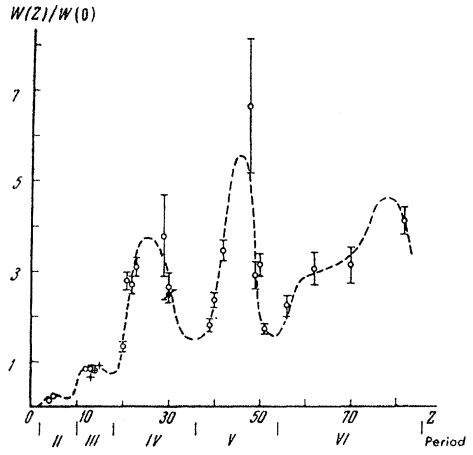

FIG. 8. The experimental capture ratios for oxides. This is Fig. 6 of Ref. 15.

To explore this periodic behavior further, we note that the general character of the electronegativity is that it increases as one goes from group I toward group VIII of the elements. Slight irregularities occur in the transition region, but Pauling's list shows that an increase in electronegativity of the positive ion results in a lower ionic character I; thus I *decreases* as one goes up from group I. If we recall now that the parameter Z_f is the number of valence electrons, N (in the common oxidation state) times I, and that N *increases* as the atomic number Z increases from group I, Z_f is thus a produce of an increasing and a decreasing function of Z.

We plot in Fig. 6 the dependence of the capture ratio on Z_f when all other parameters are held fixed; e.g., we vary Z_f for one compound like MgO. We see that the ratio of capture increases as Z_f is increased. This can be understood as the result of the increase of the attractive part of the potential in the positive ion (and the decrease in the negative ion) when Z_f is raised. (The Madelung potential is not big enough to offset this trend, since it is comparable to the attractive part coming from Z_f only near the surface of the ion.)

In Fig. 7, we plot the ratio of capture for oxides versus the atomic number Z of the position ion, for the second, third, and fourth periods. We assumed a linear Z-dependent background and normalized at $Z=12$ (Mg) on the plot. We see that it goes through a maximum in each of these periods, corresponding to the maxima of Z_f, as speculated before. On the same plot we put in some of the experimental points. Zinov's plot (Fig. 6 of Ref. 15), containing most of the experimental points, is reproduced in Fig. 8. Before comparing the calculated and the experimental points in Fig. 7 we must bear in mind that we have neglected all other changes (e.g., crystal structure) except that coming from the parameter Z_f, and also a linear Z law is assumed as the background (which is roughly correct experimentally). In addition, we assumed in the calculation that the dependence of the capture ratio on Z_f is similar to that given on Fig. 6, i.e., for $Z=12$. However, Fig. 6 is based on a fictitious variation of the parameter Z_f, and although we believe that the monotonic (or nearly so) behavior of the function is general, we do not expect that the actual behavior itself is correct for all Z. Also, we assumed that the total effect of Z_f can be represented by the change in the positive ion only, and yet we know that Z_f affects both the positive and the negative ions. Finally, we have to consider the oxidation states of the element since the curve in Fig. 7 is based on the "common oxidation states"[14] of the elements and is therefore not necessarily the states of the elements in the compounds of the experiments.

A comparison of the calculated and the experimental capture ratios for oxides (Figs. 7 and 8) shows that there is good agreement for $Z \lesssim 20$. This is to be expected since the calculation is normalized at $Z=12$. We notice, however, that even for high Z's the discrepancy is not gross. Qualitatively, the oscillatory behavior of the capture ratio with the period of the periodic table and the positions of the maxima and minima agree quite well between theory and experiment especially considering the crudeness of the model. We are, therefore, led to conclude that the main features of the capture of mesons are included in this model.

ACKNOWLEDGMENTS

We would like to express our thanks to Professor E. Segré for originally interesting us in this problem and to Dr. D. Jenkins for many helpful discussions.

[15] V. G. Zinov, A. D. Koning, and A. I. Maklin, Yadern. Fiz. 2, 859 (1965) [English transl.: Soviet J. Nucl. Phys. 2, 613 (1966)].